

MAGNETOSPHERICALLY REFLECTED WHISTLERS AS A SOURCE OF PLASMASPHERIC HISS

A. B. Draganov, U. S. Inan, V. S. Sonwalkar, and T. F. Bell

Space, Telecommunications and Radioscience Laboratory, Stanford University, Stanford, California 94305

Abstract. Ray-tracing simulations and estimates of whistler wave damping show that magnetospherically reflected whistlers can persist for $\sim 10^2$ s in a low frequency band ($f \sim 1$ kHz). The combined contribution from whistler rays produced by a single lightning flash but entering the magnetosphere at different points form a continuous hiss-like signal, as observed at a fixed point. Estimates indicate that the total whistler wave energy input into the magnetosphere from lightning discharges may maintain experimentally observed levels of magnetospheric hiss.

1. Introduction

Gyroresonant wave-electron interactions involving magnetospheric hiss has received considerable early attention [Kennel and Petcheck, 1966], due to the omnipresence of hiss within the plasmasphere. The generation mechanisms of hiss remain controversial despite extensive theoretical and experimental work. Although initial models required wave propagation parallel to the magnetic field lines for wave growth and sustenance [Thorne et al., 1979], recent experimental data show that hiss often propagates at and may originate in source regions with relatively high wave-normal angles [Lefeuvre et al., 1983; Sonwalkar and Inan, 1988]. Calculations have shown that wave growth in the magnetosphere may be not sufficient to produce the observed intensities [Huang et al., 1983], although waves propagating on selected raypaths may be amplified [Church and Thorne, 1983].

In this paper, we present an alternative and possibly complementary mechanism for the generation and sustenance of hiss. This work was stimulated by recent satellite data [Sonwalkar and Inan, 1989] showing that a hiss-like signal often follows lightning generated whistlers. The quantitative basis for our model lies in extensive ray tracing analyses of the lifetime of multiply reflected whistlers, which show that whistler rays entering the magnetosphere at a distributed set of points generate a continuum of wave energy that constitutes a signal with a hiss-like spectrum. Preliminary estimates indicate that thunderstorms worldwide inject enough wave energy into the magnetosphere to maintain the experimentally observed levels of hiss.

2. Results of Ray-tracing Calculations

Ray-tracing calculations were carried out with the Stanford VLF ray-tracing program [Inan and Bell, 1977, and references therein] using a diffusive equilibrium model for the plasmaspheric electron density consisting of a mixture of 30% H^+ and of 70% O^+ at 1000 km, with a plasma density of 500 cm^{-3} at $L=4$, a uniform plasma temperature of 2000°K , and a plasmopause location at $L=6$. The initial wave energy was

assumed to enter the magnetosphere at 400 km altitude at 16 discrete frequencies ranging from 500 Hz to 4.0 kHz over a finite range of geomagnetic latitudes ($40^\circ < \lambda_m < 51^\circ$) and with initial spread in wave-normal angles (ψ) of up to $\pm 10^\circ$ around vertical, corresponding to inhomogeneity in the transverse direction with a scale of $k_\perp^{-1} \sim 10^2$ km (k_\perp is the transverse wavevector), which can result from mild irregularities in the lower ionosphere [Sonwalkar et al., 1984].

In the presence of typical plasmaspheric density and magnetic field gradients, ψ approaches the resonance cone angle (ψ_r) after several magnetospheric reflections (at the lower hybrid frequency) with the wave energy thereafter propagating almost along the magnetic field line [Edgar, 1976]. Due to this behaviour, rays injected at different λ_m and ψ have the tendency to settle down at the same L -shell after several reflections [Jasna et al., 1990], with the L -value depending only on wave frequency. A typical raypath is shown in Figure 1 to illustrate this behaviour. We note that due to this convergent feature of the ray trajectories, calculation errors do not grow during the integration.

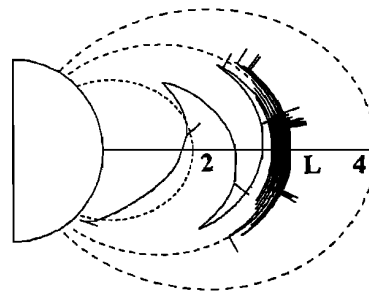


Fig. 1. A typical trajectory of a 1 kHz whistler ray originating at 46° latitude with initial wave vector (\vec{k}) orientation along the magnetic field line. Small segments at the trajectory show the orientation of the wave vector.

The dots in Figure 2a represent the L value at the equatorial plane crossings of the trajectories of 1 kHz rays (that have entered the medium at different λ_m and with different ψ as discussed above) as a function of hop number (i.e., the number of reflections that the ray has undergone). Trajectories with different initial parameters propagate at different L -shells during the first 15-20 hops but eventually settle down to propagation at $L \simeq 2.8$. The group time delay Δt_g (as observed at the equatorial plane) for the same set of trajectories is given in Figure 2b and show substantial variation among them. This diversity in Δt_g is the property which leads to the formation of a nearly continuous signal as observed at a given point.

The total lifetime of a wave packet propagating along any of the ray paths is limited by wave damping. Relatively straightforward evaluation of the potential for damping can be made via the Landau resonant electron energy \mathcal{E} corresponding to the raypath locations of Figure 2a,b, which is plotted in Figure

Copyright 1992 by the American Geophysical Union.

Paper number 91GL03167
0094-8534/92/91GL-03167\$03.00

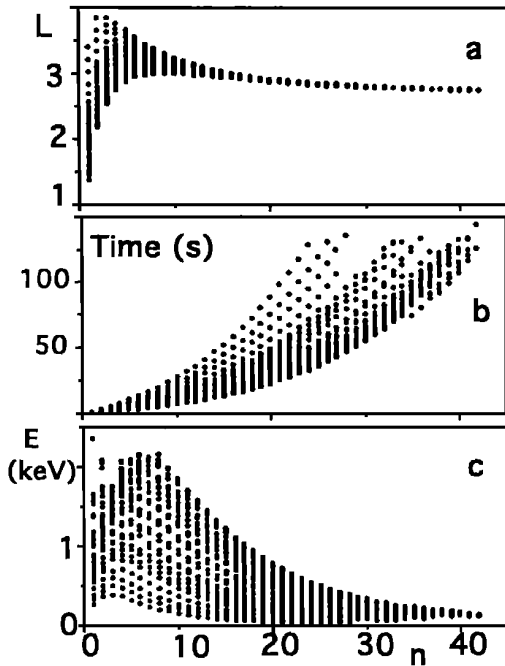


Fig. 2. Results of ray tracing simulation for whistler mode waves originating from a single lightning flash. The rays with 1 kHz frequency were injected with initial ψ of $\pm 10^\circ$ around vertical and initial λ_m of 40° to 51° at 400 km altitude. (a) L values for rays at the equatorial plane versus hop number n . (b) Group time delay at the equatorial plane versus n . (c) Landau resonant electron energy at the equatorial plane versus n .

2c. We note that \mathcal{E} approaches the thermal electron energies (i.e., < 10 eV) only after several tens of hops, indicating that the damping along the raypaths would be small. In our analyses, the ray-tracing calculations are carried out up to the point where $\mathcal{E}=40$ eV, so that we can safely assume Landau damping to be negligible (also see Section 3 below).

Any frequency component of the continuous noise-like signal observed at a given time at any point is formed by a ray of that frequency that arrives to the observation point at that time. The large number of ray trajectories analyzed represent a sample of waves originating at the same lightning discharge, but differing in λ_m , initial ψ and frequency, and can be used to determine the frequency-time spectrum to be observed by a satellite located at several selected regions in the magnetosphere.

Figure 3 shows frequency-time diagrams for various observation regions that are reconstructed by means of tracking the time at which rays at each of the 16 discrete frequencies (ranging from 500 Hz to 4.0 kHz), injected into the magnetosphere under different conditions (λ_m , ψ), cross the observation region. Here, each dot represents an equatorial plane crossing in the selected region of an individual ray path. The 36 trajectories used for each frequency allow for enough resolution without having the dots overlap in Figure 3. The observation regions were chosen as $1.90 < L < 1.91$, $2.82 < L < 2.83$, and $3.47 < L < 3.48$ to have a radial extent small enough so that the spectra would be similar to that observed on a spacecraft, but large enough to contain a reasonable number of raypaths. As observed in a fixed region, signals from consequent hops do overlap after the first several hops and, over

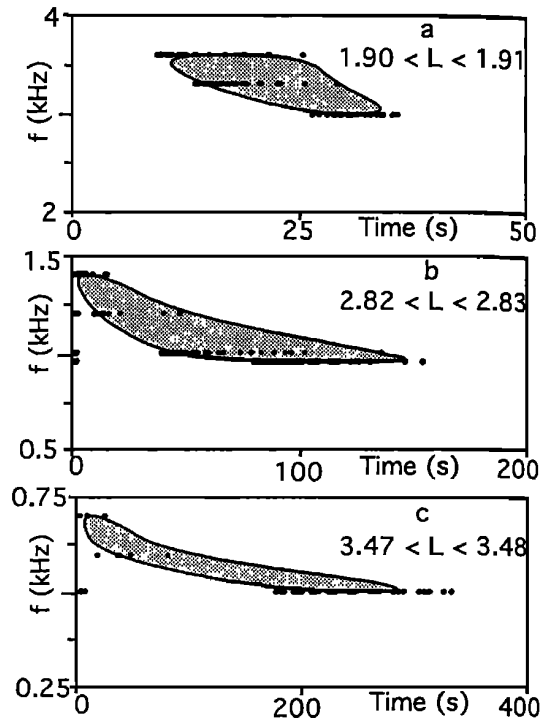


Fig. 3. Frequency-time diagram for rays crossing the equatorial plane at observation regions in the magnetosphere defined as (a) $1.90 < L < 1.91$, (b) $2.82 < L < 2.83$, and (c) $3.47 < L < 3.48$. Initial ψ and λ_m of the rays are the same as in Figure 2. Sixteen discrete frequencies ranging from 500 Hz to 4.0 kHz were considered. The highlighted envelope constitutes the continuous hiss-like spectrum that would be observed on a satellite.

time, the subset of rays that arrive at the observation region form an enduring hiss-like signal with distinctive upper and lower frequency cutoffs. These continuous signals are well defined by our finite set of points and are sketched in Figure 3 as shaded areas. Discrete magnetospherically reflected whistlers formed by first several hops of the initial whistler [Edgar, 1976] are not shown in Figure 3 since we emphasize long-time scale behavior. These discrete whistlers play a significant role in the evolution of the hiss-like signal, since the discrete whistler components at lower frequencies penetrate to higher L -shells during the first several hops, and a hiss-like spectrum develops ~ 10 s after the initial lightning flash.

From Figures 3a through 3c we can see that higher frequency signals would be observed at lower L -shells ($f \sim 3.5$ kHz at $L \simeq 1.90$ compared to $f \sim 0.6$ kHz at $L \simeq 3.47$). The spectral widths of the signals ranges from ~ 1 kHz for the highest observation region ($L=3.47$) (Figure 3a) to $\sim 10^2$ Hz for the lowest L -shell one ($L=1.90$) (Figure 3c). The duration (limited by the Landau wave damping condition of $\mathcal{E} > 40$ eV) of the continuous signals caused by a single lightning flash, ranges from ~ 30 s for $f \sim 3.5$ kHz at $L=1.90$ (Figure 3a) to ~ 200 s for $f \sim 0.6$ kHz observed at $L=3.47$ (Figure 3c).

In this work, we limited ourselves to 2D raytracing calculations. 3D effects would cause the waves to diverge up to several degrees in longitude during each hop [Cairo and Lefeuvre, 1986], so that the wave energy may be distributed over a broad range of longitudes during several tens of hops. The longitudinal divergence of hiss-like signal from one light-

ning flash would lead to lower intensity at the source longitude compared to the case of 2D propagation, but the signal can now be observed over a broader range of longitudes. Thus, the hiss observed at a given longitude might potentially be contributed to by thunderstorms at different longitudes. Since the average rate of lightning occurrence on a global scale is $\sim 100 \text{ s}^{-1}$ [Uman, 1987], and the energy injected by each lightning can be stored up to $\sim 10^2 \text{ s}$, a continuous hiss signal can potentially be sustained by wave energy from thunderstorms. In view of the longitudinal divergence of the whistler energy, there may be no strong correlation between regions of hiss enhancements and local regions of thunderstorm activity. Since the general trend is that low-frequency (high L -shell) signals from a single lightning flash persist more than high-frequency (low L -shell) signals, lightning is a more likely contributor to the sustenance of hiss at frequencies $f < 1 \text{ kHz}$ on L -shells of ~ 3 -4, in qualitative agreement with reported observations of plasmaspheric hiss [Thorne et al., 1973].

3. Wave Damping and Sustenance of Hiss

According to the results presented above the magnetosphere can act as an efficient resonator to retain whistler-mode wave energy injected into the medium from lightning discharges. The damping of whistler mode waves and the rate of pumping of the resonator by whistlers from lightning should determine the prevailing levels of plasmaspheric hiss.

A. Wave Damping

In constructing the spectra of Figure 3, the hiss-like signals formed by whistlers were limited in duration by considering only those portions of each individual raypath for which $\mathcal{E} > 40 \text{ eV}$. This value is much higher than the thermal electron energy in the plasmasphere ($\sim 1 \text{ eV}$) [S-300 Experimenters, 1979], so that if the electron distribution does not have a high energy tail, lightning generated hiss may persist for even longer than is indicated in Figure 3.

To assess the interaction with a high-energy tail of the electron distribution that might sometimes be present, we consider a simple model of a $\sim 5 \text{ eV}$ Maxwellian plasma. Figure 4 presents the whistler mode wave parameters and damping rate $\text{Im } \omega$ versus the transverse component of wavevector k_{\perp} for a fixed value of $\text{Re } \omega = 2\pi \times 1273 \text{ rad/s}$. Plasma parameters considered correspond to $L = 2.82$. Figure 4 shows that the whistler mode waves with $k \approx 2 \times 10^{-2} \text{ m}^{-1}$ (corresponding to $\mathcal{E} \approx 40 \text{ eV}$ for $k_{\parallel} \approx 0.1 k_{\perp}$) do not damp significantly (Im

$\omega < 10^{-3} \text{ s}^{-1}$), indicating that the hiss-like signals in Figure 3 can endure even longer if the magnetospheric plasma has no high-energy tail. During periods of high magnetospheric activity, an energetic tail of the electron distribution can form and lead to a higher damping rate. Thus, our model predicts hiss to be more prevalent during quiet magnetospheric conditions, again in qualitative agreement with reported observations [Thorne et al., 1973].

B. Sustenance of Hiss by Wave Energy from Lightning

We first consider the total energy of hiss in the magnetosphere using both the observed spectral density of $U \sim 1 \text{ pT/Hz}^{1/2}$ [Thorne et al., 1973], and wave parameters as predicted by our ray-tracing. For $k_{\parallel} \approx 10^{-1} \cdot k \approx 5 \times 10^{-3} \text{ m}^{-1}$, and using quantities $R = (cB/E) \approx 1$ and $\sin \alpha \approx 10^{-3}$ (α being the angle between \vec{B} and \vec{E}) which are plotted in Figure 4 versus k_{\perp} , and a total hiss bandwidth of $\Delta f \approx 3 \times 10^2 \text{ Hz}$, we obtain the wave energy density to be $\rho = c^2 U^2 \Delta f \sin \alpha / (\eta R V_g) \approx 5 \times 10^{-17} \text{ Joules/m}^3$, where $\eta = 377 \Omega$ is the intrinsic impedance of the free space. We assume that the wave group velocity V_g , $V_g \approx \omega/k_{\parallel}$, as appropriate for whistler waves with $\psi \approx \psi_r$ and $k_{\perp} \gg k_{\parallel}$. The total hiss wave energy in the volume \mathcal{V} of the magnetosphere defined by $2 < L < 4$ ($\sim 2 \times 10^{22} \text{ m}^3$) would then be $W = \rho \mathcal{V} \approx 10^6 \text{ Joules}$. In the context of our model of hiss formation, this energy would be dissipated over a time of $\tau \approx 10^2 \text{ s}$ (Figure 3), so that the rate of energy loss is $Q_h \approx (W/\tau) \approx 10^4 \text{ Joules/s}$. This value is to be compared to the rate at which lightning flashes can pump the hiss.

Based on satellite observations of VLF signals from ground-based sources [Rastani et al., 1985], we assume the diameter of the region where the energy from a lightning flash enters the ionosphere to be $\sim 10^3 \text{ km}$. During the first hop, quasi-longitudinal whistler rays do not change their longitude considerably [Cairo and Lefeuvre, 1986]. Therefore, we can assume $\sim 10^3 \text{ km}$ to be the dimension in longitude of the whistler ray spot at the equatorial plane after the first hop. However, the dimension of the whistler ray spot in the radial direction can be as large as $\sim 10^4 \text{ km}$ (see Figure 2a). Using a typical whistler intensity of $B_w \approx 3 \text{ pT}$, the duration of whistler in the equatorial plane of $\tau_w \approx 2 \times 10^{-1} \text{ s}$, and a typical refractive index of $\mu \approx 30$, we estimate the total whistler wave energy projected to the magnetic equatorial plane by a single lightning flash to be $W_w \approx c^2 B_w^2 \tau_w S / (\eta \mu) \approx 1.5 \times 10^2 \text{ Joules}$. Using the average global lightning rate of $\sim 10^2 \text{ s}^{-1}$ [Uman, 1987], we find the total whistler power available to 'pump' hiss to be $Q_w \approx 1.5 \times 10^4 \text{ Joules/s}$. Since Q_w is comparable to Q_h , lightning generated whistlers on a global scale can potentially provide enough energy to maintain levels of plasmaspheric hiss with spectral density of $1 \text{ pT/Hz}^{1/2}$.

4. Summary and Discussion

Our results suggest that lightning generated whistler wave energy can develop into plasmaspheric hiss via multiple reflections and that thunderstorm activity on a global scale may be sufficient to support observed hiss levels.

This new model of plasmaspheric hiss generation and sustenance is based on the fact that whistler waves generated by lightning can persist in the magnetosphere for a long time, undergoing multiple magnetospheric reflections and effectively

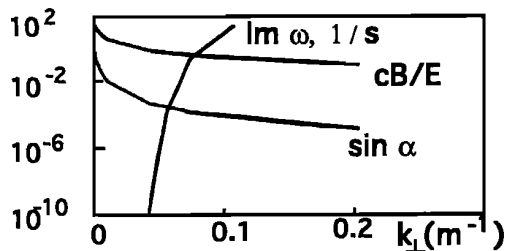


Fig. 4. Wave damping rate ($\text{Im } \omega$), longitudinal component of wave vector (k_{\parallel}), sine of the angle between \vec{E} and \vec{B} ($\sin \alpha$), and (cB/E) ratio for $\text{Re } \omega = 2\pi \times 1273 \text{ rad/s}$ at $L = 2.82$. A Maxwellian plasma with 5 eV temperature was assumed.

being 'stored' by the magnetospheric resonator. Quantitative modeling of whistlers propagating in magnetospheric plasma with a high-energy non-exponential tail was reported by Huang *et al.* [1983], who showed that waves originating with an initial intensity greater than the thermal level can propagate a considerable distance before damping out, and that the total growth/damping rates for such whistlers are low. Further, Church and Thorne [1983] have shown that the natural incoherent emissivity of the magnetospheric plasma is unlikely to be the source of hiss but that once the emission is established, it can be maintained. Our results show that magnetospherically reflected whistlers can lead to the formation of continuous hiss-like signals with durations of up to $\sim 10^2$ sec at lower frequencies (~ 1 kHz). Based on these estimates, we suggest that lightning activity alone can be a source for magnetospheric hiss without any necessary amplification of whistler mode waves as long as the whistler damping rates are relatively low. The hiss-like signals produced by magnetospherically reflected whistlers have properties that are in qualitative agreement with reported experimental data on plasmaspheric hiss, in particular, with Dynamic Explorer-1 observations of the features (upper and lower cutoff frequencies and their variation with time) of hiss which often follow whistlers [Sonwalkar and Inan, 1989].

According to our model, most plasmaspheric hiss would be observed at high ψ , in agreement with experimental results [Lefeuvre *et al.*, 1983; Sonwalkar and Inan, 1988]. Some reported observations of hiss with small ψ [Parrot and Lefeuvre, 1986] may be due either to whistler mode ducting or to components that are guided by the plasmopause [Church and Thorne, 1983]. Although our model implies that hiss would always occur above the lower hybrid frequency (f_{LHR}), spectral components of hiss below f_{LHR} are sometimes observed [e.g., Church and Thorne, 1983, see Figure 1]. It is possible that this effect may be due to relatively large Doppler shifts that result from the high ψ . For $k \sim 10^{-1} \text{ m}^{-1}$, the Doppler shift would be $\sim 10^2$ Hz.

Acknowledgments. We thank our colleagues in the STAR Laboratory for helpful discussions. This research was supported by NASA grant NAG5-476 to Stanford University.

References

- Cairo, L., and F. Lefeuvre, Localization of sources of ELF/VLF hiss observed in the magnetosphere: Three-dimensional ray tracing, *J. Geophys. Res.*, **91**, 4352, 1986.
- Church, S. R., and R. M. Thorne, On the origin of plasmaspheric hiss: Ray path integrated amplification, *J. Geophys. Res.*, **88**, 7941, 1983.
- Edgar, B. C., The upper and lower frequency cutoffs of magnetospherically reflected whistlers, *J. Geophys. Res.*, **81**, 205, 1976.
- Huang, C. Y., C. K. Goertz, and R. R. Anderson, A theoretical study of plasmaspheric hiss generation, *J. Geophys. Res.*, **88**, 7927, 1983.
- Inan, U. S., and T. F. Bell, The plasmopause as a VLF wave guide, *J. Geophys. Res.*, **82**, 2819, 1977.
- Jasna, D., U. S. Inan, and T. F. Bell, Equatorial gyroresonance between electrons and magnetospherically reflected whistlers, *Geophys. Res. Lett.*, **17**, 1865, 1990.
- Kennel, C. F., and H. E. Petschek, Limit on stably trapped particle fluxes, *J. Geophys. Res.*, **71**, 1, 1966.
- Lefeuvre, F., M. Parrot, L. R. O. Storey, and R.R. Anderson, Wave distribution functions for plasmaspheric hiss observed on board ISEE 1, *Tech. Note LPCE/6*, Lab. de Phys. et chim. de l'Environ., Orleans, France, 1983.
- Parrot, M., and F. Lefeuvre, Statistical study of the propagation characteristics of ELF hiss observed on GEOS-1, inside and outside the plasmopause, *Annal. Geophysicae*, **4**, 363, 1986.
- Rastani, K., U. S. Inan, and R. A. Helliwell, DE-1 observations of Siple transmitter signals and associated sidebands, *J. Geophys. Res.*, **90**, 4128, 1985.
- S-300 Experimenters, Measurements of electric and magnetic wave fields and of cold plasma parameters on-board GEOS-1. Preliminary results, *Planet. Space Science*, **27**, 317, 1979.
- Sonwalkar, V. S., T. F. Bell, R. A. Helliwell, and U. S. Inan, Direct multiple path magnetospheric propagation: A fundamental property of nonducted VLF waves, *J. Geophys. Res.*, **89**, 2823, 1984.
- Sonwalkar, V. S., and U. S. Inan, Wave normal direction and spectral properties of whistler mode hiss observed on the DE 1 satellite, *J. Geophys. Res.*, **93**, 7493, 1988.
- Sonwalkar, V. S., and U. S. Inan, Lightning as an embryonic source of VLF hiss, *J. Geophys. Res.*, **94**, 6986, 1989.
- Thorne, R. M., E. J. Smith, R. K. Burton, and R. E. Holzer, Plasmaspheric hiss, *J. Geophys. Res.*, **78**, 1581, 1973.
- Thorne, R. M., S. R. Church, and D. J. Gorney, On the origin of plasmaspheric hiss: the importance of wave propagation and the plasmopause, *J. Geophys. Res.*, **84**, 5241, 1979.
- Uman, M. A., *The Lightning Discharge*, 377 pp, Academic Press, Orlando, U.S.A., 1987.
- A. B. Draganov, U. S. Inan, V. S. Sonwalkar, and T. F. Bell, Space, Telecommunications And Radioscience Laboratory, Department of Electrical Engineering/SEL, Stanford University, Stanford, CA 94305.

(Received: October 16, 1991;
accepted: December 4, 1991.)